Mathematical Biosciences 271 (2016) 19–28

Contents lists available at ScienceDirect

Mathematical Biosciences

journal homepage: www.elsevier.com/locate/mbs

A two-clones tumor model: Spontaneous growth and response to treatment

Ilaria Stura[a,*], Ezio Venturino[b], Caterina Guiot[a]

[a] Dipartimento Neuroscienze, Università di Torino, Corso Raffaello 30, 10125 Torino, Italy
[b] Dipartimento di Matematica "Giuseppe Peano", Università di Torino, via Carlo Alberto 10, 10123 Torino, Italy

ARTICLE INFO

Article history:
Received 10 June 2015
Revised 23 September 2015
Accepted 16 October 2015
Available online 30 October 2015

Keywords:
Mathematical model
Tumor growth
Gompertz
PUN

ABSTRACT

The paper aims at providing a general theoretical frame bridging the macroscopic growth law with the complex heterogeneous structure of real tumors. We apply the "Phenomenological Universality" approach to model the growth of cancer cells accounting for "populations", which are defined not as biologically predefined cellular ensemble but as groups of cells behaving homogeneously with respect to their position (e.g. primary or metastatic tumor), growth characteristics, response to treatment, etc. Populations may mutually interact, limit each other their growth or even mutate into another population. To keep the description as simple and manageable as possible only two populations are considered, but the extension to a multiplicity of cell populations is straightforward.

Our findings indicate that the eradication of the metastatic population is much more critical in the presence of mutations, either spontaneous or therapy-induced. Furthermore, a treatment that eradicates only the primary tumor, having a low kill rate on the metastases, is ultimately not successful but promotes a "growth spurt" in the latter.

1. Introduction

Tumor is a very inhomogeneous system of cells [1] dynamically interacting and adapting to their environment. Normally two or more cell populations coexist, e.g. the primary tumor and one or more secondary ones, generated by cells of the primary tumor which moved to lymph nodes or distant organs. Adaptation to different environments normally modifies the cells characteristics, originating a different cell population. To account for any heterogeneity among cells, due to whatever cause or nature, different cell populations are considered. The transformation of a given population into another one is termed mutation whenever the phenotypic modifications reflect genetic alterations. Sometimes such mutations may be induced or modulated in response to therapies (see [2] in case of the prostate cancer). As a matter of fact, primary tumors are normally treated by surgical eradication or radical radio therapy. When unsuccessful, tumor seeds may survive generating a local recurrence (whose cells may be somewhat different from their progenitor, adding a new cell population into the picture). At the same time, in order to prevent or, more often, to control distant tumor spread, systemic therapies are delivered, generally called chemo-therapies. Nowadays, also hormone therapies are very common to contrast the growth of hormone-sensitive tumors, like breast and prostate cancer. In this last case it is well known that, after an initial reduction of the tumor volume, the growth of hormone-resistant cells will finally induce an almost uncontrollable tumor saturation [2]. Any realistic model should therefore take into account the appearance of therapy-induced cell mutations.

The key question in the modeling strategy is how strong the interplay among different cell populations must be. Since they are part of the same organism, a "minimal" hypothesis states that they share the same overall energetic and physical resources. Since the total tumor carrying capacity is limited, it is therefore reasonable to assume that the growth of both cell populations is constrained [3,4]. However, several authors (see for instance [5,6]) have speculated about the possibility that the whole tumor (i.e primary, nodes and metastases) behaves as a "coherent body". Experimental evidences of enhanced proliferation of the dormant secondary tumors following the surgical excision of the primary one have been shown in both animal [7,8] and human [9,10] models. A recent model of [3] shows that the effect of primary tumor resection on the growth of bone metastases is not always favorable: since large tumors limit the resources available

* Corresponding author. Tel.: +39 0116708198.
E-mail addresses: ilaria.stura@unito.it (I. Stura), ezio.venturino@unito.it (E. Venturino), caterina.guiot@unito.it (C. Guiot).

http://dx.doi.org/10.1016/j.mbs.2015.10.014

for the growth of smaller ones, the resection of the primary tumor may trigger the proliferation of dormant tumors by promoting their vascularization and growth.

The biological mechanisms underlying the above macroscopic findings are still debated. The simultaneous production of growth hormones and angiogenic factors as well as of their inhibitors by the primary tumor, and their different stability (normally the inhibitors have a longer lifetime) may explain the successful control of the metastatic progression until the primary tumor is present. Also the post-surgery wound healing processes and the resulting local and systemic inflammation may be responsible for secondary tumor growth [11,12].

We investigate here the equilibrium conditions of two asymmetrical cell populations, paying close attention to their stability or instability, which are assumed to predict the successful cure or the fatal evolution of the tumor. The parameter conditions ensuring the stable configuration, i.e. the stop of the tumor growth, are outlined in detail.

The paper is organized as follows. In Section 2 the governing equations for the cell populations growth, with or without therapeutic interventions, are presented. In Section 3 two non-mutating populations are investigated, assuming as mutual interplay the constraint on the total carrying capacity, accounting for the geometrical restrictions and the overall environmental conditions, such as growth factor release and energetic resources. The response to therapies is investigated in Section 4. Section 5 considers the spontaneous or therapy-induced emergence of a mutated population. In Section 6 the results are collected in a phase-space diagram encompassing real clinical situations occurring in a large population of patients at different stages of tumor evolution. We focus on possible practical applications as the case of recurrent prostate cancer, where previously prostectomized patients are treated with Androgen Deprivation Therapy (ADT). Such therapy is very effective on the initially predominant hormone-sensitive cancer cells, but promotes a mutation into non-hormone sensitive cells and finally fails in controlling tumor proliferation. A final discussion concludes the paper.

2. The model

The recently proposed Phenomenological Universalities (PUN) approach [13–16] actually includes most of the growth models proposed in the past within a single mathematical frame: they range from simple exponential to logistics and Gompertzian growth, to the ontogenetic model of [17]. PUN was successfully applied to describe the tumor multi-passage transplant in mice [6], external stresses limiting tumor invasiveness [18], multi-cellular tumor spheroids [19] as well as to simulate the response to selected therapies [20]. Applications to other growth phenomena, such as human height from birth to maturity [21] show that the model may easily include "growth spurts"provided a "piece-wise" formulation is used. In this setting, each time interval is characterized by its own specific parameter values. Extensions of PUN to multiple cells populations have been proposed as well, e.g. proposing a "vector" PUN model [22].

The PUN approach describes tumor growth in a very general way, see [15,16] for details:

$$\begin{cases} \dfrac{dN(t)}{dt} = c(t)N(t) \\ \dfrac{dc(t)}{dt} = \displaystyle\sum_{i=0}^{n} \beta_i c^i \end{cases} \tag{1}$$

where N is the cancer cells population, $c(t)$ is the growth rate function and n is the degree of the Taylor expansion. This approach generalizes the most used equations in population growth, in fact: in the case $n = 0$, $c(t)$ constant, N grows following an exponential law; for $n = 1$, it follows a Gompertzian law and for $n = 2$ a West/logistic growth law, [23].

2.1. U_0 – Malthus growth law

The first approximation of tumor growth is the exponential law; in fact, at an initial stage, tumor cells duplicate very fast with a fixed doubling time (i.e. the time in which the cancer mass doubles) which estimates the rate of the exponential growth.

Using PUN notation, we see that, for $n = 0$, from (1) the derivative of c is a constant; assuming it vanishes, $\beta_0 = 0$, it follows that $c(t) = c_0$ which in turn implies $N(t) = e^{c_0 t}$, upon integration of the first (1). For $c_0 > 0$, the model exhibits an unbounded population growth. However, real tumors cannot expand indefinitely because of physical constraints. Thus, in the subsequent sections we will not consider this unrealistic case anymore.

2.2. U_1 – Gompertzian growth law

This function describes the tumor development more realistically. Indeed, following an initial exponential unrestricted phase, due to lack of nutrients and space the tumor population growth progressively slows down until finally the tumor population attains its carrying capacity. The mathematics reflects the biological processes, i.e. the cancer core becomes hypoxic and necrotic while the proliferating tumor border may reach some physical barrier such as tissue or bones and it stops growing. The dynamic system, in the $U1$ case, is:

$$\begin{cases} \dfrac{dN(t)}{dt} = c(t)N(t) \\ \dfrac{dc(t)}{dt} = \beta_1 c + \beta_0 \end{cases}$$

Integrating the second equation by separation of variables, setting $\beta_0 = 0$, $c_0 = e^{-\beta_1 t_0}\beta_1^{-1}$, $\beta = \beta_1 < 0$ and then substituting $c(t)$ into the first one we have:

$$\frac{dN(t)}{dt} = c_0 e^{\beta t} N(t) \tag{2}$$

whose solution is:

$$N(t) = N_0 e^{\frac{c_0}{\beta}(e^{\beta t}-1)}. \tag{3}$$

where β is inversely proportional to the tumor carrying capacity and c_0 denotes the growth rate. Note that in this case the carrying capacity depends on the initial condition N_0.

To emphasize the role of the carrying capacity, Eq. (3) can be rewritten as:

$$N(t) = N_\infty e^{ze^{-rt}} \tag{4}$$

where $N_\infty = \lim_{t\to\infty} N(t) = N_0 e^{-\frac{c_0}{\beta}}$ is the carrying capacity and r the exponential growth rate. We can easily transform (3) into (4) back and forth by setting $r = -\beta$, $N_\infty = N_0 e^{-\frac{c_0}{\beta}}$ and $z = \frac{c_0}{\beta}$.

2.3. U_2 – West growth law

West and collaborators have published their allometric theory to give a robust physical foundation to the empirical relationship between the basal metabolic rate and the 3/4 power of the mass observed in all living beings (Kleiber scaling law, [24]) This formalism has been extended by [15] for tumors. In addition to the carrying capacity, a second independent parameter relating the cellular metabolic energy and the energy required for duplication comes into play. Also this function could be derived by the PUN approach, in fact for $n = 2$ we have:

$$\frac{dc(t)}{dt} = \beta_0 + \beta_1 c + \beta_2 c^2.$$

This is a very general equation that defines a class of functions; in particular, choosing $\beta_2 = -\frac{1}{4}$, $t_0 = 0$ and β_1 inversely proportional to

the carrying capacity N_∞, N is seen to follow the West growth law:

$$\frac{dN(t)}{dt} = AN^{\frac{3}{4}}\left[1 - \sqrt[4]{\frac{N}{N_\infty}}\right] \tag{5}$$

where A is the ratio between the cellular metabolic rate B_c (which depends on the cell line) and the energy E_c required to form a new cell. As shown by [25], this parameter could be easy estimated by the observed growth time scale $\tau = \frac{4E_c}{B_c}$.

In the following sections we will use an equivalent notation for U_2 for which an analytical solution is readily found. Assuming $N_\infty = (\beta_0\beta_2\beta_1^{-1} - 1)^{\frac{1}{4}}$, $\beta_1 < 0$ and $A = -4\beta_1 N_\infty^{\frac{1}{4}}$ we have:

$$c(t) = \frac{\beta_0}{\left(1 + \frac{\beta_0\beta_2}{\beta_1}\right)e^{-\beta_1 t} - \frac{\beta_0\beta_2}{\beta_1}}$$

$$N(t) = N_\infty\left[1 - \left(1 + \sqrt[4]{\frac{N_0}{N_\infty}}\right)e^{-\frac{1}{4}\frac{At}{\sqrt[4]{N_\infty}}}\right]^4. \tag{6}$$

where N_∞ is the carrying capacity and A corresponds to the initial growth rate. Note that it affects the time at which the function reaches the limiting value but it does not influence the final value itself.

3. The two weakly interacting populations model

We assume the cancer mass to be composed by different groups of cells (or populations), distinguished either genetically (e.g. two or more clones of the same tumor) or epigenetically (e.g. hypoxic/oxic cells at the center/at the edge of the mass). To describe the tumor using the PUN approach, we denote by N_1 and by N_2 the two populations. Assuming that the two populations are independent of each other, the system becomes:

$$\begin{cases} \frac{dN_1(t)}{dt} = c_1(t)N_1(t) \\ \frac{dN_2(t)}{dt} = c_2(t)N_2(t) \end{cases} \tag{7}$$

and the solutions are independent and each population grows on its own.

In realistic contexts the carrying capacities of the populations are in fact constrained by physical and energetic restrictions, because the total carrying capacity at most equals the maximum volume available for the tumor to expand (e.g. the intestine for the primary tumor plus the liver for the metastasis) or is limited by the amount of nutrients that cancer cells could use to grow. As shown by [3], the primary tumor often uses most of the total nutrients precluding the growth of micro-metastases, but whenever the primary tumor is eradicated, metastases exhibit a sudden growth spurt.

The constraint is expressed by the condition $N_{\infty,1} + N_{\infty,2} = N_\infty$, which in turn implies a relationship among the growth parameters. In practice, as is common in the literature, [3], in the models that follow we implement the restriction by introducing a new parameter ϵ providing an extra degree of freedom. We could interpret this parameter as a measure of the metabolic rate increment in response to particularly favorable growth conditions. It also expresses an additional growth rate for the second population. We thus obtain

$$\begin{cases} \frac{dN_1(t)}{dt} = c_1(t)N_1(t) \\ \frac{dN_2(t)}{dt} = c_2(t)N_2(t) + \epsilon N_2(t). \end{cases} \tag{8}$$

Note also that the populations proliferate differently during tumor growth: in the early stage $N_1(t) \gg N_2(t)$ because N_1 is expanding and the second population is a minor clone; if N_1 is instead the primary tumor and N_2 is a metastasis, then $N_1(t) \ll N_2(t)$ because in the new site the cancer cells can freely proliferate.

4. The two populations model with treatment

In order to eradicate or reduce the volume of the tumor, the majority of the diagnosed primary cancers are treated by radical surgery or radio-therapy. These treatments are administered in a relatively short time (1–40 days). To prevent and/or control secondary tumors hormone- and chemo-therapies are instead prescribed for a longer time span (months-years).

As it often occurs, we assume that the two populations respond to treatments differently. In particular let us assume that cell population 1 is very sensitive to the therapy while population 2 is either less sensitive or not sensitive at all to it. This situation resembles the clinical cases when in the same tumor mass a clone resistant to hormone therapy coexists with another one sensitive to it, or when two separated masses are differently treated, i.e. the primary tumor with radio-therapy and the metastasis with hormone/chemo-therapy. The system (7) becomes:

$$\begin{cases} \frac{dN_1}{dt} = c_1(t)N_1 - d_1(t)N_1 \\ \frac{dN_2}{dt} = c_2(t)N_2 - d_2(t)N_2 \end{cases} \tag{9}$$

where $d_1(t)$ and $d_2(t)$ are the treatment kill rates on the populations N_1 and N_2 respectively. In principle, d_1 and d_2 could be functions of time to account for different times of treatments and one- or multi-shot therapies. For sake of simplicity, in the following computation we will assume d_1 and d_2 to be constants with $d_1 \gg d_2$, stating that N_1 is more sensitive and d_2 is negligible if the treatment of N_2 is ineffective.

4.1. U_1 case

In case of the Gompertzian growth law we have $c_1(t) = c_1 e^{\beta_1 t}$, $c_2(t) = c_2 e^{\beta_2 t}$ with c_1, c_2, β_1 and β_2 having constant values. The analytical solutions are:

$$N_1 = N_{0,1}e^{\frac{c_1}{\beta_1}e^{\beta_1 t} - d_1 t - \frac{c_1}{\beta_1}} = N_{\infty,1}e^{-\frac{d_1}{r_1}}e^{\log(N_{0,1}/(N_{\infty,1}exp(-d_1/r_1)))e^{-r_1 t}}$$

$$N_2 = N_{0,2}e^{\frac{c_2}{\beta_2}e^{\beta_2 t} - d_2 t - \frac{c_2}{\beta_2}} = N_{\infty,2}e^{-\frac{d_1}{r_1}}e^{\log(N_{0,2}/(N_{\infty,2}exp(-d_2/r_2)))e^{-r_2 t}}$$

For the equilibrium points we have $c_i(t) = d_i$, $i = 1, 2$, from which the times to reach the equilibria are obtained, $t_1^* = \beta_1^{-1}\log\left(d_1 c_1^{-1}\right)$ and $t_2^* = \beta_2^{-1}\log\left(d_2 c_2^{-1}\right)$, with $c_i < d_i$ and $t_i^* > 0$, $i = 1, 2$. In the limit, N_i tends to zero whenever $d_i > 0$, $i = 1, 2$.

Rewriting the system using Eq. (4) and accounting for the maximal total carrying capacity for the tumor, recall (8), we have:

$$\begin{cases} \frac{dN_1(t)}{dt} = -r_1 N_1(t)\log\frac{N_1}{N_{\infty,1}} - d_1 N_1(t) \\ \frac{dN_2(t)}{dt} = -r_2 N_2(t)\log\frac{N_2}{N_{\infty,2}} - d_2 N_2(t) + \epsilon N_2(t). \end{cases} \tag{10}$$

The value of ϵ corresponding to the fixed total carrying capacity is given in Table 1. The solutions are respectively

$$N_1(t) = N_{\infty,1}e^{-\frac{d_1}{r_1}}e^{\log(N_{0,1}/(N_{\infty,1}exp(-d_1/r_1)))e^{-r_1 t}}$$

$$N_2(t) = N_{\infty,2}e^{-\frac{d_2}{r_2}}e^{\log(N_{0,2}/(N_{\infty,2}exp(-(d_2-\epsilon)/r_2)))e^{-r_2 t}}.$$

In the limit, they tend respectively to $N_{\infty,1}^* = N_{\infty,1}\exp(-\frac{d_1}{r_1})$ and to $N_{\infty,2}^* = N_{\infty,2}\exp(-\frac{d_2-\epsilon}{r_2})$; note that the carrying capacities are modified (see Figs. 1 and 2). Empirically, population 1 can be considered eradicated when $d_1 \geq 10r_1$. In the general case, the critical value of m depends both on r_1 and $N_{\infty,1}$. Note that using the initial assumption ($d_2 \ll d_1$) the best scenario (death of both populations) is not attained so easily, since $d_2 \gg \epsilon + r_2$.

Table 1
U_1 case: modified carrying capacities and interaction constant in the different scenarios.

Model	$N^*_{\infty,1}$	$N^*_{\infty,2}$	ϵ
(7)	$N_{\infty,1}$	$N_{\infty,2}$	0
(9)	$N_{\infty,1}e^{\frac{-m}{r_1}}$	$N_{\infty,2}e^{\frac{\epsilon+m\frac{N^*_{\infty,1}}{N^*_{\infty,2}}}{r_2}}$	$r_2\log\left(\frac{N_\infty - N_{\infty,1}e^{-\frac{m}{r_1}}}{N_{\infty,2}}\right) - m\frac{N^*_{\infty,1}}{N^*_{\infty,2}}$
(12)	$N_{\infty,1}e^{-\frac{d_1}{r_1}}$	$N_{\infty,2}e^{-\frac{d_2-\epsilon}{r_2}}$	$r_2\log\left(\frac{N_\infty - N_{\infty,1}e^{-\frac{d_1}{r_1}}}{N_{\infty,2}}\right) - d_1$
(15)	$N_{\infty,1}e^{\frac{-(m+d_1)}{r_1}}$	$N_{\infty,2}e^{-\frac{d_2-\epsilon-m\frac{N^*_{\infty,1}}{N^*_{\infty,2}}}{r_2}}$	$r_2\log\left(\frac{N_\infty - N_{\infty,1}e^{-\frac{m+d_1}{r_1}}}{N_{\infty,2}}\right) - m\frac{N^*_{\infty,1}}{N^*_{\infty,2}} - d_1$

4.2. U_2 case

In case of the West law we present the alternative formulation of the model used in (5). The system becomes:

$$\begin{cases} \dfrac{dN_1}{dt} = A_1 N_1^{\frac{3}{4}}\left(1 - \sqrt[4]{\dfrac{N_1}{N_{\infty,1}}}\right) - d_1 N_1 \\ \dfrac{dN_2}{dt} = A_2 N_2^{\frac{3}{4}}\left(1 - \sqrt[4]{\dfrac{N_2}{N_{\infty,2}}}\right) - d_2 N_2 + \epsilon N_2(t). \end{cases} \tag{11}$$

Again, the value of ϵ fixing the total carrying capacity is reported in Table 2. Unfortunately, the analytical solutions are not easily manageable, but we can study the limits of the two solutions that have the form $N_i^* = (N_{\infty,i}^{-\frac{1}{4}} + d_i A_i^{-1})^{-4}$, $i = 1, 2$. Note that in the simplest case without treatment the limit corresponds to the carrying capacity $N_{\infty,i}$, without any dependencies on the growth factor. This limit depends on A_i, that is the strength of the tumor growth (see Fig. 3).

5. The two populations model with mutation

If one of the two populations, e.g. the first one, is a less resistant and/or is composed by a less aggressive clone than the other, it tends to mutate to better adapt to the environment. The velocity of the mutation depends on the effective advantage experienced by the mutated population: if it is not so marked, e.g. it has a slightly different growth rates, the mutation could be slow, otherwise the first population tends to mutate very rapidly, as it may occur when a therapy is very effective against the first population but not against the second one. We describe this situation as follows:

$$\begin{cases} \dfrac{dN_1(t)}{dt} = c_1(t)N_1(t) - mN_1(t) \\ \dfrac{dN_2(t)}{dt} = c_2(t)N_2(t) + mN_1(t) \end{cases} \tag{12}$$

where, assuming no leaking, m represents the cell mutation rate from the first to the second clone.

5.1. U_1 case

In case of the Gompertzian growth law we have $c_1(t) = c_1 e^{\beta_1 t}$, $c_2(t) = c_2 e^{\beta_2 t}$ with c_1, c_2, β_1 and β_2 constants. The analytical solutions are:

$$N_1 = N_{\infty,1} e^{-r_1 e^{\frac{t}{N_{\infty,1}} - mt + r_1}},$$

$$N_2 = e^{c_2 e^{\beta_2 t} - c_2}\left(m\int^t e^{-\frac{c_2}{\beta_2}e^{\beta_2\lambda} + \frac{c_2}{\beta_2}} N_1(\lambda)d\lambda + C\right).$$

In the limit, N_1 tends to zero when $m > 0$. Since the behavior cannot be described analytically, the numerical evaluation shows that the limit of N_2 depends on $c_1 c_2 (\beta_1\beta_2)^{-1}$.

Rewriting the system using Eq. (4) and imposing a fixed carrying capacity N_∞ we have:

$$\begin{cases} \dfrac{dN_1(t)}{dt} = -r_1 N_1(t)\log\dfrac{N_1}{N_{\infty,1}} - mN_1(t) \\ \dfrac{dN_2(t)}{dt} = -r_2 N_2(t)\log\dfrac{N_2}{N_{\infty,2}} + mN_1(t) + \epsilon N_2(t) \end{cases} \tag{13}$$

where ϵ is given in Table 1. For simplicity, we now impose no constraint ($\epsilon = 0$). In this case

$$N_1(t) = N_{\infty,1} e^{-\frac{m}{r_1}} e^{\log(N_{0,1}/(N_{\infty,1}exp(-m/r_1)))e^{-r_1 t}}$$

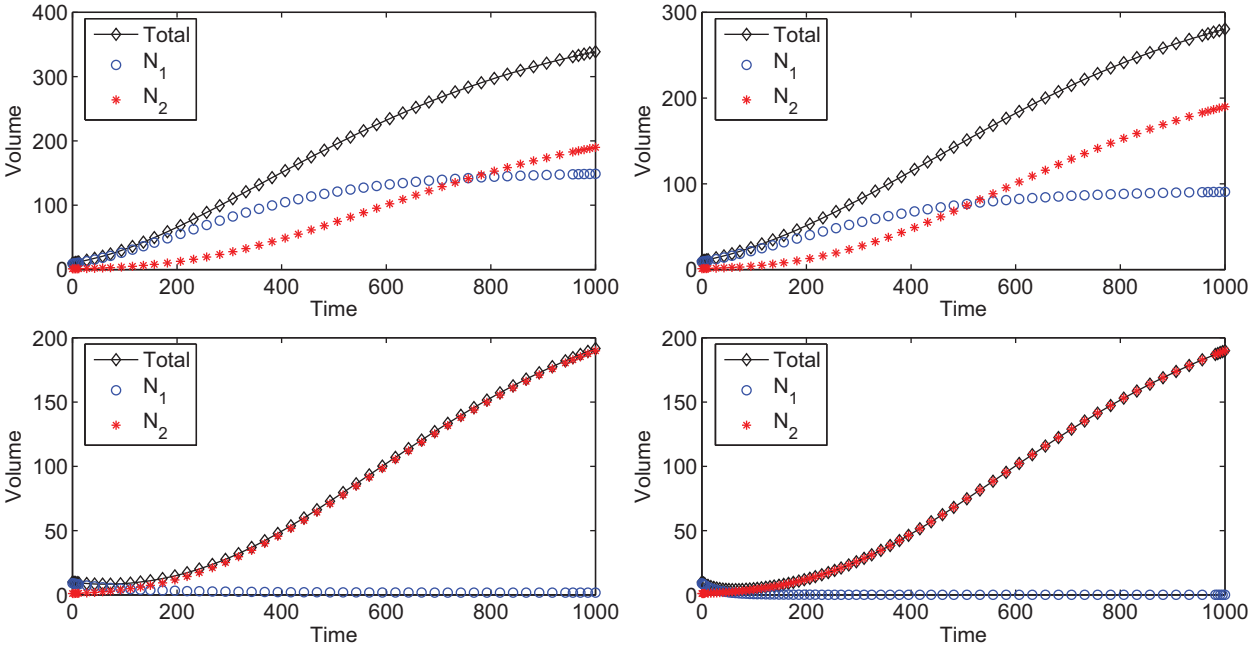

Fig. 1. Treatment in the U_1 case. Changing the kill rate parameter d_1 we can observe the coexistence of the two populations (top frames) or the extinction of the first one (bottom frames). Top right frame: the kill rate is smaller than the growth rate ($r_1 = 0.005$, $d_1 = 0.0025$). Top left frame: kill and growth rates are equal ($r_1 = 0.005$, $d_1 = 0.005$). Bottom frames: the kill rate is larger than the growth rate; $r_1 = 0.005$, $d_1 = 0.025$ (left), $r_1 = 0.005$, $d_1 = 0.05$ (right).

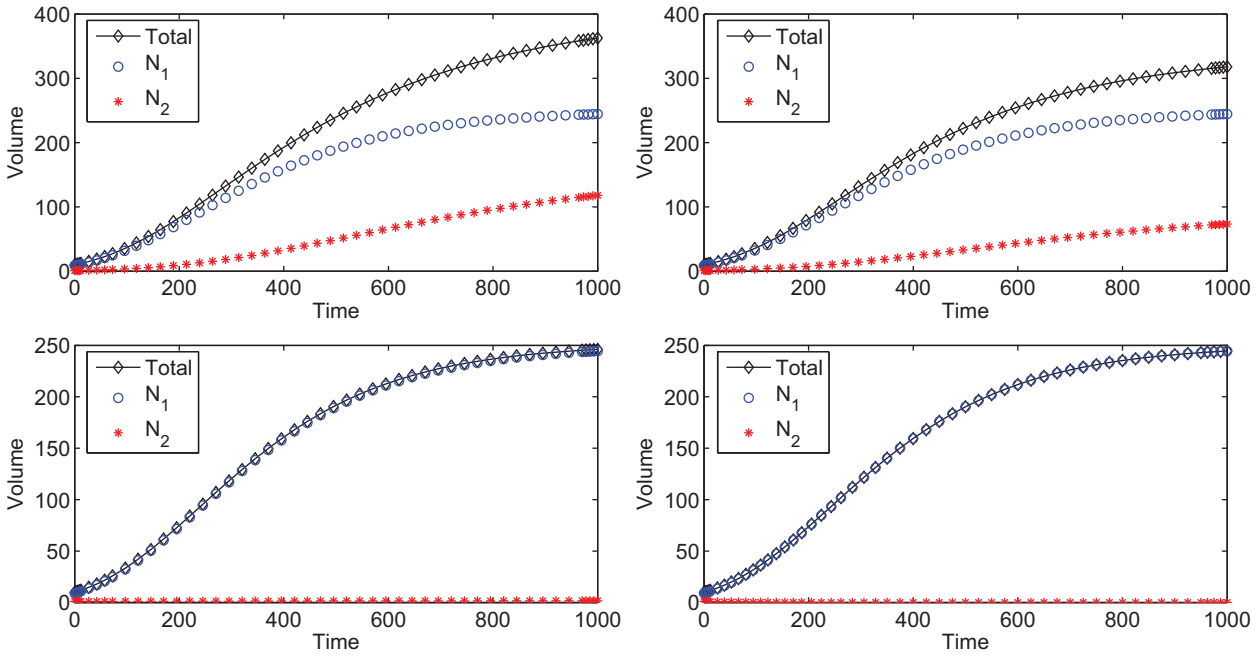

Fig. 2. Treatment in the U_1 case. Changing the kill rate parameter d_2 we can observe the coexistence of the two populations (top frames) or the extinction of the second one (bottom frames). Top right frame: the kill rate is smaller than the growth rate ($r_1 = 0.003$, $d_1 = 0.0015$). Top left frame: kill and growth rates are equal ($r_1 = 0.003$, $d_1 = 0.003$). Bottom frames: the kill rate is larger than the growth rate; $r_1 = 0.003$, $d_1 = 0.015$ (left), $r_1 = 0.003$, $d_1 = 0.03$ (right).

Table 2
U_2 case: modified carrying capacities and interaction constant in the different scenarios.

Model	$N^*_{\infty,1}$	$N^*_{\infty,2}$	ϵ
(6)	$N_{\infty,1}$	$N_{\infty,2}$	0
(11)	$\left(\frac{1}{N_{\infty,1}^{1/4}} + \frac{d_1}{A_1}\right)^{-4}$	$\left(\frac{1}{N_{\infty,2}^{1/4}} + \frac{d_2-\epsilon}{A_2}\right)^{-4}$	$d_2 + A_2\left(\frac{1}{N_{\infty,2}^{1/4}} - \frac{1}{(N^*-N_1^*)^{1/4}}\right)$
(14)	$\left(\frac{1}{N_{\infty,1}^{1/4}} + \frac{m}{A_1}\right)^{-4}$	$\left(\frac{(\frac{A}{N_{\infty,2}^{1/4}}-\epsilon)N_2^* - mN_1^*}{A_2}\right)^{\frac{4}{3}}$	$-m\frac{N_1^*}{N^*-N_1^*} + A_2\left(\frac{1}{N_{\infty,2}^{1/4}} - \frac{1}{(N^*-N_1^*)^{1/4}}\right)$
(17)	$\left(\frac{1}{N_{\infty,1}^{1/4}} + \frac{m+d_1}{A_1}\right)^{-4}$	$\left(\frac{(\frac{A}{N_{\infty,2}^{1/4}}+d_2-\epsilon)N_2^* - mN_1^*}{A_2}\right)^{\frac{4}{3}}$	$d_2 - m\frac{N_1^*}{N^*-N_1^*} + A_2\left(\frac{1}{N_{\infty,2}^{1/4}} - \frac{1}{(N^*-N_1^*)^{1/4}}\right)$

so that it tends to $N^*_{\infty,1} = N_{\infty,1}e^{-\frac{m}{r_1}}$, hence the first population will vanish if and only if $e^{-\frac{m}{r_1}}$ is close to 0, which entails $m \gg r_1$. Again a sufficient condition for the disappearance of population 1 is $m \geq 10r_1$, i.e. the mutation must be very effective. In the general case, the critical value of m depends both on r_1 and $N_{\infty,1}$. The modified carrying capacity of the second population is $N^*_{\infty,2} = N_{\infty,2}\exp\left(-\frac{m}{r_2}\frac{N^*_{\infty,1}}{N^*_{\infty,2}}\right)$, which is not an explicit formula (see Fig. 4). Provided $N_{\infty,1} \ll N_{\infty,2}$ the condition $m \ll r_2$ is not strong enough to ensure the population growth.

In the phase plots (Fig. 5) we can see that the system tends to the equilibrium point $(N^*_{\infty,1}, N^*_{\infty,2})$ both in case of extinction of the first population and in case of coexistence of the two clones.

Imposing the constraint $N_{\infty,1} + N_{\infty,2} = N_\infty$, and then

$$\epsilon = r_2 \log\left[\left(N_\infty - N_{\infty,1}\exp\left(-\frac{m}{r_1}\right)\right)N_{\infty,2}^{-1}\right] - m\frac{N^*_{\infty,1}}{N^*_{\infty,2}},$$

and the second population could increase (if $\epsilon > 0$) or decrease (if $\epsilon < 0$) depending on the initial carrying capacities of both populations and on the mutation rate.

5.2. U_2 case

As in the treatment case, the analytical solutions are not so easy to manage, but we can study the limits of the two solutions N_1 and N_2 using the notation (5); the system becomes:

$$\begin{cases} \dfrac{dN_1}{dt} = A_1 N_1^{\frac{3}{4}}\left[1 - \sqrt[4]{\dfrac{N_1}{N_{\infty,1}}}\sim\right] - mN_1 \\ \dfrac{dN_2}{dt} = A_2 N_2^{\frac{3}{4}}\left[1 - \sqrt[4]{\dfrac{N_2}{N_{\infty,2}}}\sim\right] + mN_1 \end{cases} \tag{14}$$

The limits for t tending to infinity are then found:

$$N_1^* = \left(\frac{1}{N_{\infty,1}^{1/4}} + \frac{m}{A_1}\right)^{-4}, \quad N_2^* = \left(\frac{mN_1^*}{\frac{A_2}{N_{\infty,2}^{1/4}} - \frac{A_2}{N_2^{*1/4}}}\right)^{\frac{4}{3}}.$$

Note that N_1^* also in this case depends on the growth rate A_1, while N_2^* is strictly linked to the first one and depends on both the growth rates A_1 and A_2, on the mutation rate and on the initial carrying capacities. In Fig. 6 note also the behavior of the second population: it has a larger advantage if $A_1 > A_2$ than in the reverse case.

6. Combination of mutation and treatment

In real pathological situations the mutation could be induced by the treatment itself. Accounting for such a situation, the model

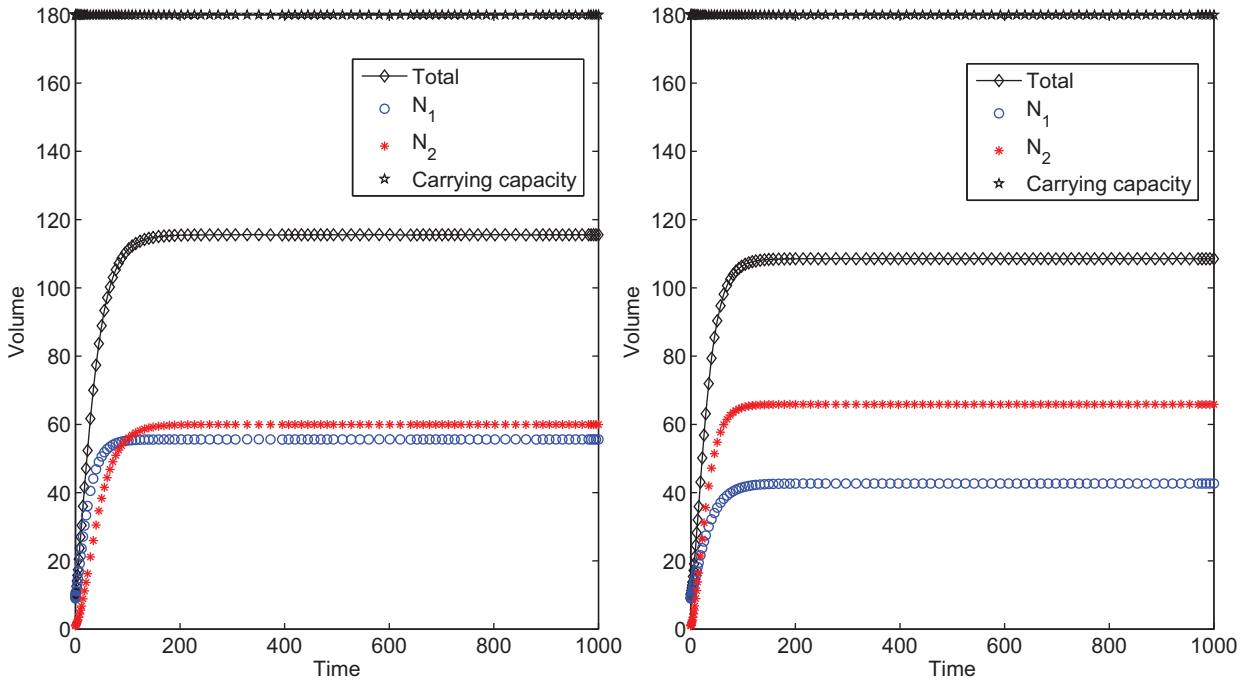

Fig. 3. An example of treatment when cells grow according to the West law. In both frames the two populations receive the same treatment ($d_1 = 0.03, d_2 = 0.01$). Note how the growth rate changes the final carrying capacities: in the left frame we take $A_1 = 0.9$ and $A_2 = 0.4$, in the right one $A_1 = 0.4$ and $A_2 = 0.9$. As a reference, we plot also the horizontal lines indicating the levels of the carrying capacities that the tumors would reach in the absence of treatment.

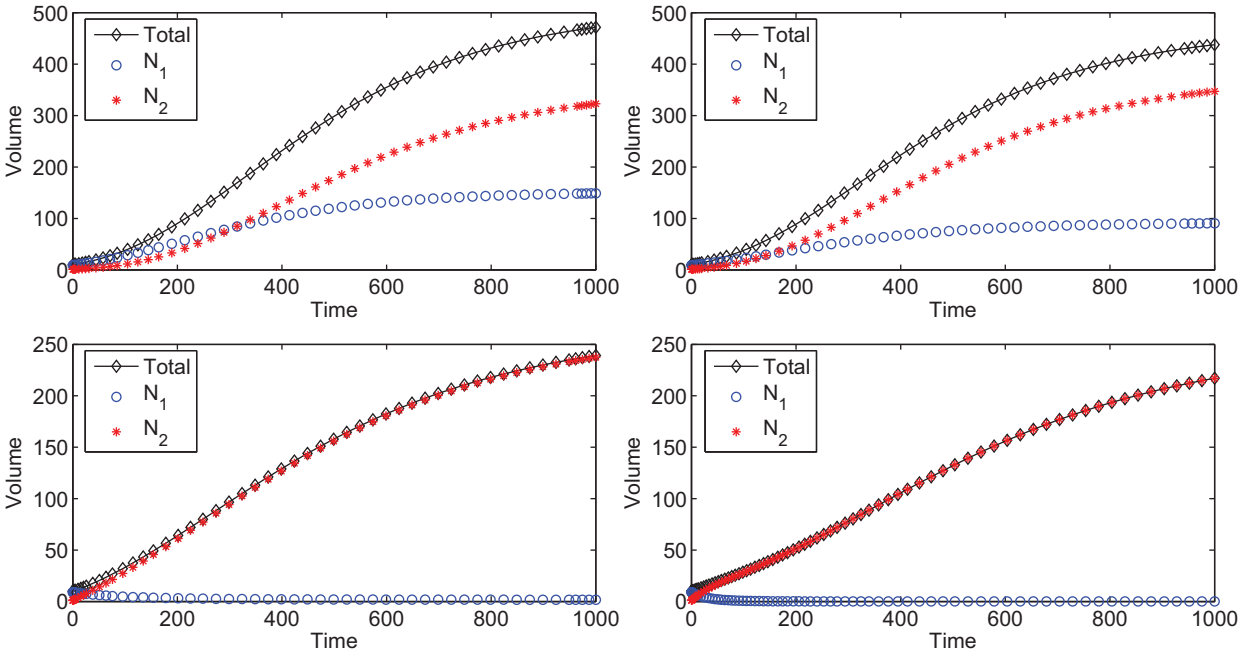

Fig. 4. Mutation in U_1 case. Changing the mutation parameter m we can observe the coexistence of the two populations (top row) or the extinction of the first one (bottom row). Top right frame: the mutation rate is smaller than the growth rate ($r_1 = 0.005, m = 0.0025$). Top left frame: mutation and growth rates are equal ($r_1 = 0.005, m = 0.005$). Bottom frames: the mutation rate is larger than the growth rate; $r_1 = 0.005, m = 0.025$ (left), $r_1 = 0.005, m = 0.05$ (right).

becomes:

$$\begin{cases} \dfrac{dN_1(t)}{dt} = c_1(t)N_1 - m(t)N_1 - d_1(t)N_1 \\ \dfrac{dN_2(t)}{dt} = c_2(t)N_2 + m(t)N_1 - d_2(t)N_2 \end{cases} \tag{15}$$

Note that we inserted a time dependence in (15) for both the mutation and kill rates: in fact, in the general case, the treatment could vary in time (e.g. cycles of different drugs) and the mutation will change along with the therapy progression (e.g. no mutation without treatment, higher mutation rate in the first period of the treatment with respect to the following cycles). To model these features we use piecewise functions with constant parameters. For example, to model three chemo-therapy cycles, we used a couple of equations like (15) during the treatment (i.e. the day of the cycle and the following day) and another couple of equations like (12), without the parameters d_i, during the days between two cycles (see Fig. 9).

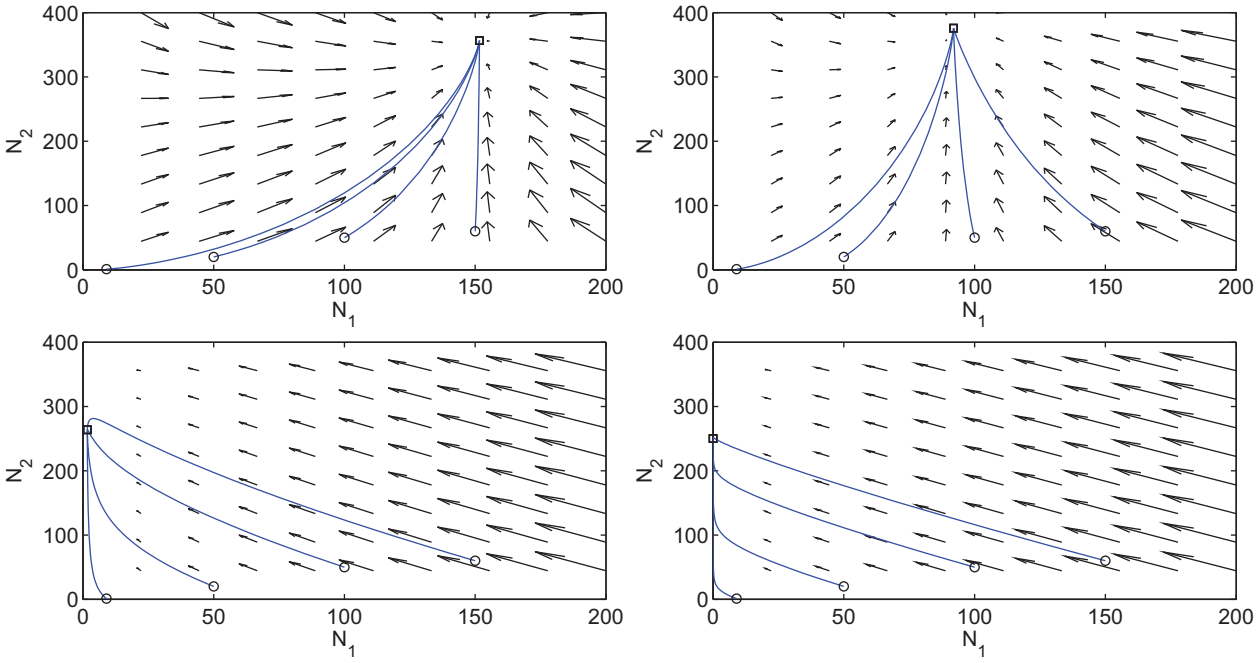

Fig. 5. Mutation in U_1 case. Phase space portraits with different mutation rates (x axis: N_1 population, y axis: N_2 population). Top right frame: the mutation does not affect the growth of both populations ($r_1 = 0.005, m = 0.0025, N^*_{\infty,1} = 151.6, N^*_{\infty,2} = 356.3$). Top left frame: the first population is visibly reduced by the mutation ($r_1 = 0.005, m = 0.005, N^*_{\infty,1} = 91.9, N^*_{\infty,2} = 375.8$). Bottom row: the first population becomes extinct while the second one thrives; $r_1 = 0.005, m = 0.025, N^*_{\infty,1} = 1.7, N^*_{\infty,2} = 263.6$ (left), $r_1 = 0.005, m = 0.05, N^*_{\infty,1} = 0.01, N^*_{\infty,2} = 250.1$ (right).

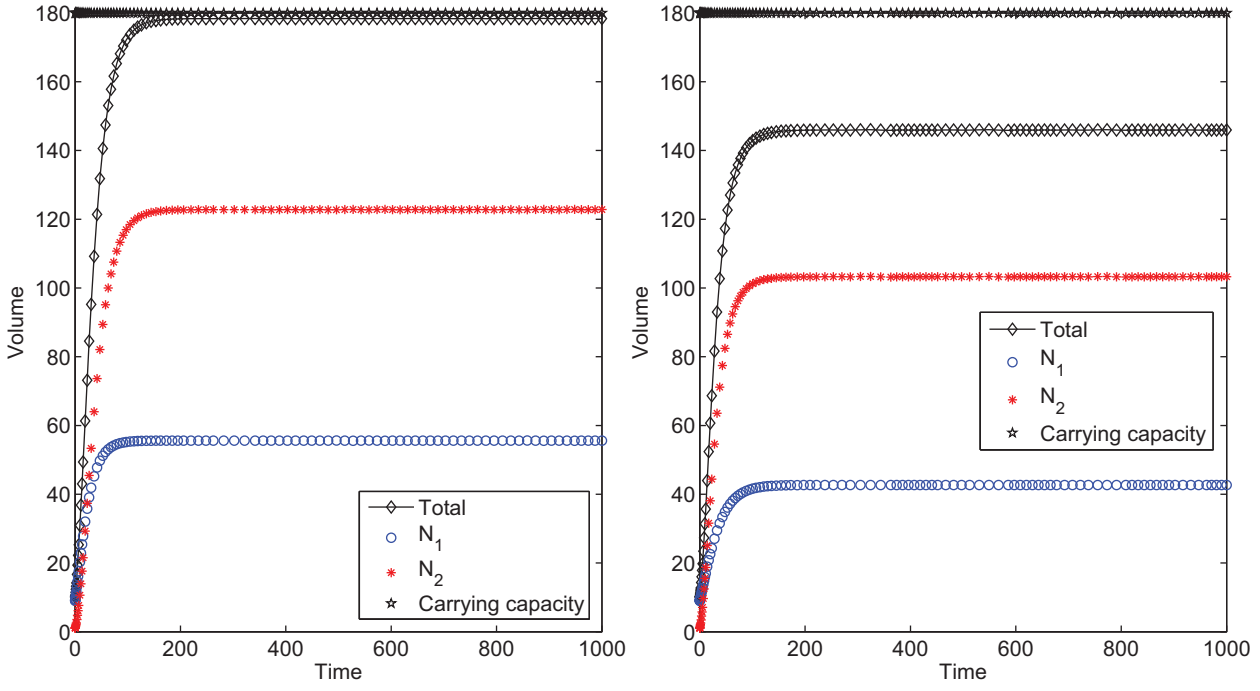

Fig. 6. An example of mutation in the West case. In both frames the two populations have the same mutation rate ($m = 0.03$). Note that population N_2 has a greater advantage in the left frame (where $A_1 = 0.6$ and $A_2 = 0.4$) than in the right one (where $A_1 = 0.4$ and $A_2 = 0.6$). As a reference, we plot also the horizontal lines indicating the levels of the carrying capacities that the tumors would reach in the absence of treatment.

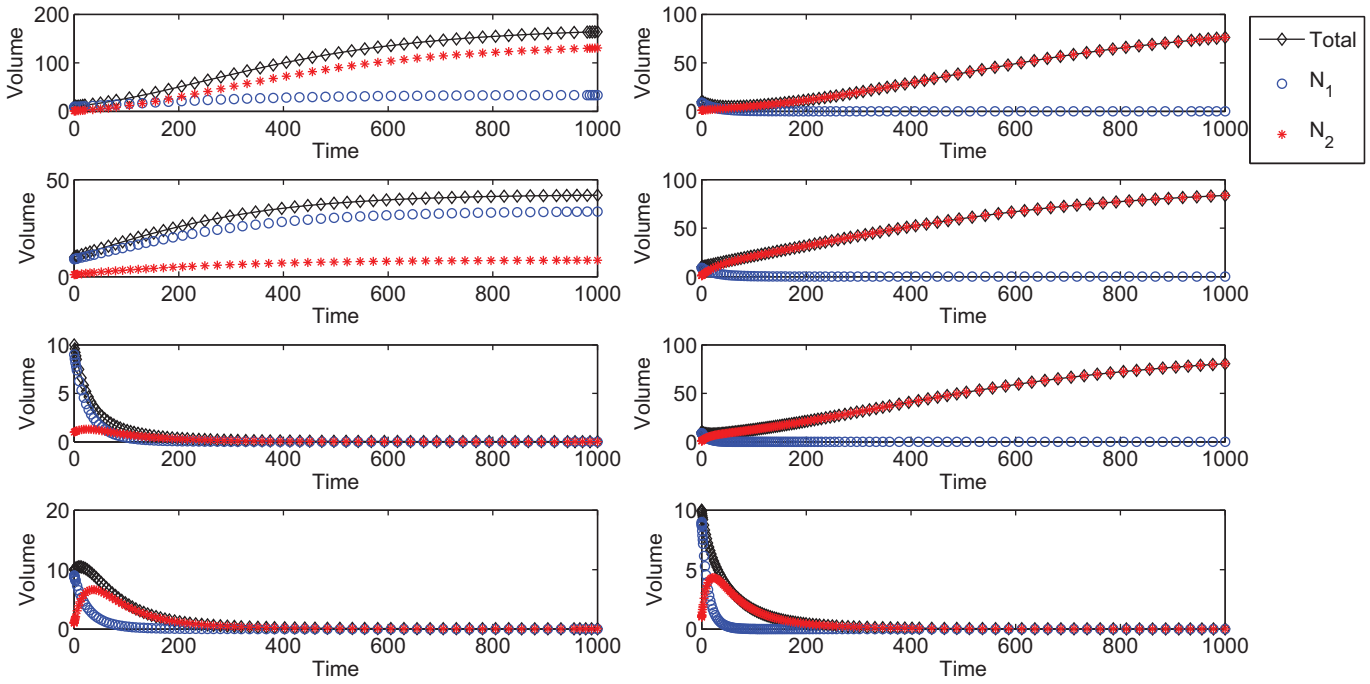

Fig. 7. Mutation and treatment in U_1 case. The parameter reference values in all frames, unless otherwise noted, are $r_1 = 0.005, r_2 = 0.003, m = 0.005, d_1 = 0.005, d_2 = 0.003$. Top row left: all parameters are at the low reference values entailing coexistence of the two populations. Top row right: high kill rate of the first population ($d_1 = 0.05$), but the second one survives; Second row left: high kill rate of the second population ($d_2 = 0.03$), the first one prevails; Second row right: high mutation rate ($m = 0.05$), only the second one thrives; Third row left: high kill rates ($d_1 = 0.05, d_2 = 0.03$), both populations are eradicated; Third row right: high kill rate of the first population and high mutation rate ($d_1 = 0.05, m = 0.05$), the first population decreases rapidly; Bottom row left: high kill rate of the second population and high mutation rate ($d_2 = 0.03, m = 0.05$), both populations vanish; Bottom row right: high kill and high mutation rates ($d_1 = 0.05, d_2 = 0.03, m = 0.05$), both populations disappear.

6.1. U_1 case

In the Gompertzian case the solutions of the system (15) are a combination of the mutation-only and treatment-only cases. The system becomes:

$$\begin{cases} \dfrac{dN_1(t)}{dt} = -r_1 N_1 \log \dfrac{N_1}{N_{\infty,1}} - mN_1 - d_1 N_1 \\ \dfrac{dN_2(t)}{dt} = -r_2 N_2 \log \dfrac{N_2}{N_{\infty,2}} + mN_1 - d_2 N_2 + \epsilon N_2. \end{cases} \tag{16}$$

The final carrying capacities are

$$N^*_{\infty,1} = N_{\infty,1} \exp\left(-\frac{m + d_1}{r_1}\right),$$

$$N^*_{\infty,2} = N_{\infty,2} \exp\left[-\frac{1}{r_2}\left(d_2 - \epsilon - m\frac{N^*_{\infty,1}}{N^*_{\infty,2}}\right)\right].$$

The tumor will be eradicated only if suitable parameter combinations involving m, d_1 and d_2 are satisfied, namely $m + d_1 \geq 10r_1$ and $d_2 - \epsilon - mN_{\infty,1}N^{-1}_{\infty,2} \geq 10r_2$. From these inequalities, if the mutation rate is low, the successful implementation of the therapy depends only on the kill rates (see Fig. 7). In the presence of a high mutation rate instead, combined with a low kill rate of the secondary tumor d_2, the main tumor is eradicated but the metastasis persists. Unfortunately, this is the worst and most common scenario: the treatment is very effective on the sensitive clone, eradicating it easily, but it promotes a "growth spurt" in the resistant clone.

6.2. U_2 case

As it occurs for the U_1 case, this is a combination of the mutation-only and the treatment-only scenarios. We can study the limits of the two solutions N_1 and N_2 using (5); the system becomes:

$$\begin{cases} \dfrac{dN_1}{dt} = AN^{\frac{3}{4}}_{\infty,1}\left(1 - \sqrt[4]{\dfrac{N_1}{N_{\infty,1}}}^{\sim}\right) - mN_1 - d_1 N_1 \\ \dfrac{dN_2}{dt} = AN^{\frac{3}{4}}_{\infty,2}\left(1 - \sqrt[4]{\dfrac{N_2}{N_{\infty,2}}}^{\sim}\right) + mN_1 - d_2 N_2 + \epsilon N_2. \end{cases} \tag{17}$$

The value of ϵ for the maximal possible total carrying capacity is given in Table 2. The limits of the populations for $t \to \infty$ are

$$N^*_1 = \left(N^{-\frac{1}{4}}_{\infty,1} + \frac{m + d_1}{A_1}\right)^{-4},$$

$$N^*_2 = \left[A_2^{-1}\left((AN^{-\frac{1}{4}}_{\infty,2} + d_2)N^*_2 - mN^*_1\right)\right]^{\frac{4}{3}}.$$

As shown in Fig. 8, the tumor growth rates A_1 and A_2 are of paramount importance to assess the final tumor volume in the case of treatment when mutation occurs. Summing the two populations equilibrium values in the two frames, we find in the right frame a smaller value than the one of the left frame. This is due to the lower value of the tumor growth rate A_1 in the right frame, although the metastasis has there a larger growth rate A_2. This behavior allows us to conjecture that a combined therapy, with chemo-therapy drugs, expressed by the d_1 and d_2 parameters, and biological therapies (i.e. hormone-therapy) which modify the metabolic cell rate, i.e. the parameters A_i, could be more effective than a massive dose of chemo-therapy drugs. Based on these simulations, we plan to investigate further the possible clinical applications and compare the treatments effectiveness by validating the model against real clinical data.

7. Discussion and conclusions

The approach of the "Phenomenological Universalities" allows a satisfactory investigation of the growth of an asymmetrical

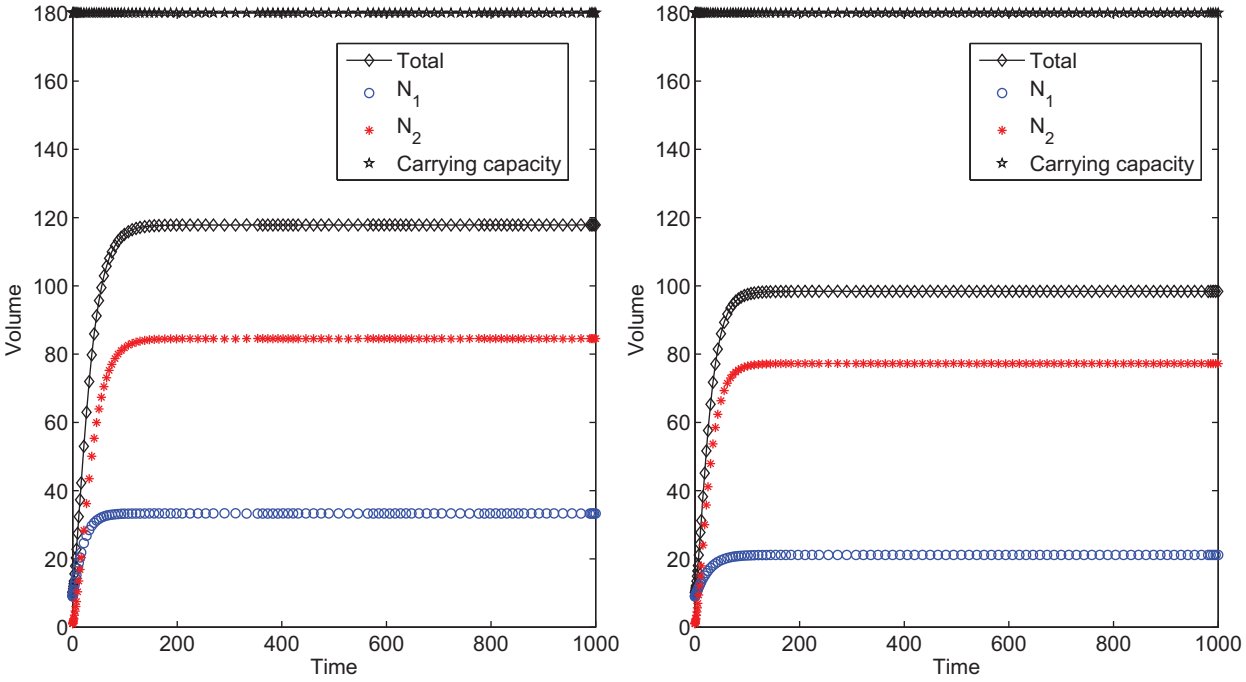

Fig. 8. An example of mutation and treatment in the West case. In both frames the two populations receive the same treatment and have the same mutation rate ($d_1 = 0.03$, $d_2 = 0.01$, $m = 0.03$). Note how the growth rate modifies the final carrying capacity: on the left $A_1 = 0.9$ and $A_2 = 0.4$, on the right $A_1 = 0.4$ and $A_2 = 0.9$. As a reference, we plot also the horizontal lines indicating the levels of the carrying capacities that the tumors would reach in the absence of treatment.

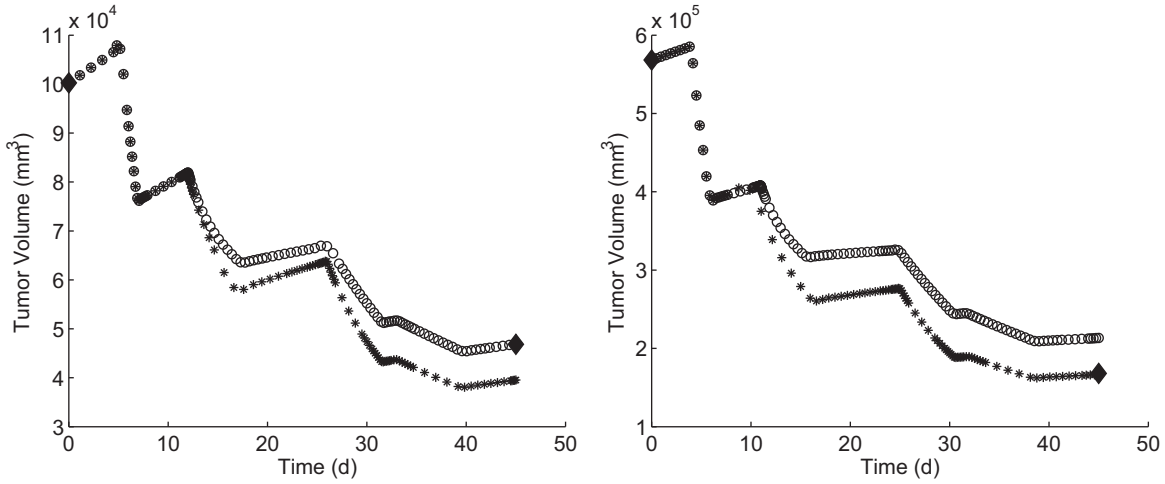

Fig. 9. Simulations of cells mutation and for the patient response to treatment in the Gompertzian case. Black rhombus are the measure of the real tumor volumes pre ($t = 0$) and after ($t = 45$) chemo-therapy. The circles represent the simulations performed with $m = 0.35$, the stars those obtained with $m = 0.09$. The patient on the left shows a bad response to treatment, since the final tumor size is related to the mutation rate $m = 0.35$; the patient on the right shows a good response to treatment since the final tumor size is instead related to $m = 0.09$.

two-population cancer. Different interactions were studied, corresponding to different clinical scenarios, i.e. the growth of both populations constrained by a fixed total carrying capacity, the response to treatments, the occurrence of spontaneous mutation and of mutations elicited by therapeutic interventions.

To model the growth of the cells populations in a manageable and realistic way we applied the Gompertzian and West functions, which have been successfully validated on various tumor scenarios, finding analytical solutions whenever possible. Numerical simulations assessed the effectiveness and role of the model parameters in the remaining cases.

In the specific case of a two-clones tumor, although effective therapies and/or a large mutation rate can reduce the primary tumor volume or the cell population which is more treatment-sensitive, our findings indicate that the eradication of the second population (e.g. metastatic population and/or less treatment-sensitive cell clones) is much more critical in the presence of spontaneous mutations and, even worse, when mutations are induced or promoted by therapies. Assuming as growth description the West law, the model emphasizes the importance of the growth rates of the cell populations to determine the final tumors size. Looking toward clinical application this approach is to be preferred, because of the biological significance of the parameter A, related to the cellular metabolic rate and duplication energy of each specific cell population. Provided such information is available for specific tumors, the West growth assumption represents an optimal model for the simulations of the tumor development and of its response to therapies. As an example of clinical application, we challenged our model against lung (Non- small cell lung, NSCL)

human cancer data (from [26]). NSCL cancer is known to be composed by two different phenotypes, i.e. hypoxic cells in the core and well oxygenated cells in the outer ring. Oxygenated cells exhibit a large growth rate but a low resistance to chemo-therapy; hypoxic cells, on the contrary, have a low growth rate but a larger resistance to chemo-therapy. In the database we chose, growth and kill rates, initial and final volumes after therapy as well as growth and drug kill rates were available. We tested our model using two scenarios: $m = 0.35$ (bad response to the treatment) and $m = 0.09$ (good response to the treatment). Unfortunately, since only the final tumor volume is available and not the two single populations (large colored dot in Fig. 9), we cannot evaluate the actual value of the mutation rates.

As far as the limitations and weaknesses of the model are concerned, two points have to be focused: 1) Timescales and actual tumor volumes cannot be desumed by the model unless the input parameter are quantitatively estimated on clinical or biological data, because the model is intrinsically non related to empirical data but to scale-free parameter and equations; 2) to realistically account for the huge number of mutations taking place during tumor growth, which differs from patient to patient, a large number of different interacting populations should be considered. Modeling $n > 2$ interacting populations is a possible future development, but numerical approaches will be necessary instead of the more direct and intuitively effective analytical ones.

Work is in progress toward the application of the model to relapsed prostate cancer in patients who underwent radical prostatectomy and are treated with Androgen Deprivation Therapy, which is known to trigger a mutation from hormone dependent to hormone resistant cancer cells. The follow-up and clinical data of some hundreds of relapsed patients contained in the EUREKA1 database [27] is being investigated in order to assess a reasonable range of values for the model parameters.

In conclusion, the model presented here could be an useful starting point for simulating different treatment scenarios and, provided a careful validation of the parameter values is carried on extensive clinical database, it may help in the preliminary estimation of the expected effectiveness of different therapeutic approaches.

Acknowledgments

This research has been funded by the European Union Seventh Framework Programme ($FP7/2007 - 2013$) under grant agreement n. 600841.

References

[1] M. Shackleton, E. Quintana, E.R. Fearon, S.J. Morrison, Heterogeneity in cancer: Cancer stem cells versus clonal evolution, Cell 138 (5) (2009) 822–829.
[2] T. Portz, Y. Kuang, J. Nagy, A clinical data validated mathematical model of prostate cancer growth under intermittent androgen suppression therapy, AIP Adv. 2 (1) (2012) 1–15.
[3] L. Hanin, S. Bunimovich-Mendrazitsky, Reconstruction of the natural history of metastatic cancer and assessment of the effects of surgery: Gompertzian growth of the primary tumor, J.Theor. Biol. 247 (2014) 47–58.
[4] I. Stura, D. Gabriele, C. Guiot, Modeling prostate cancer within chic, Minerva Urol. Nefrol. 1 (1) (2015) 97–98.
[5] A.K. Laird, Dynamics of tumour growth: Comparison of growth rates and extrapolation, Brit. J. Cancer 19 (1965) 278–291.
[6] A. Gliozzi, C. Guiot, P. Delsanto, A new computational tool for the phenomenological analysis of multipassage tumor growth curves, Plo SOne 4 (2009) e5358.
[7] M. Baum, M. Chaplain, A. Anderson, M. Douek, J. Vaidya, Does breast cancer exist in a state of chaos? Eur. J. Cancer 35 (1999) 886–891.
[8] M. Retsky, W. Demicheli R.and Hrushesky, M. Baum, I. Gukas, Surgery triggers outgrowth of latent distant disease in breast cancer: an inconvenient truth? Cancers 2 (2010) 305–337.
[9] P. Lange, K. Hekmat, G. Bosl, B. Kennedy, E. Fraley, Accelerated growth of testicular cancer after cytoreductive surgery, Cancer 45 (1980) 1498–1506.
[10] T. Tsunemi, S. Nagoya, M. Kaya, S. Kawaguchi, T. Wada, T. Yamashita, S. Ishii, Postoperative progression of pulmonary metastasis in osteosarcoma, Clin. Orthop. Related Res. 407 (2003) 159–166.
[11] F. Balkwill, A. Mantovani, Inflammation and cancer: back to virchow? Lancet 357 (2001) 539–545.
[12] M. Retsky, W. Demicheli R.and Hrushesky, P. Forget, M. DeKock, I. Gukas, R. Rogers, M. Baum, V. Sukhatme, J. Vaidya, Reduction of breast cancer relapses with perioperative non-steroidal anti-inflammatory drugs: new findings and a review, Curr. Med. Chem. 20 (2013) 4163–4176.
[13] P. Delsanto, Universality of Nonclassical Nonlinearity with applications to NDE and Ultrasonics, SpringerNorton and Co., New York, 2007.
[14] P. Delsanto, C. Guiot, A. Gliozzi, Scaling, growth and cyclicity in biology: a new computational approach, Theor. Biol. Med. Model. 5 (2008), doi:10.1186/1742-4682-5-5.
[15] C. Guiot, P. Degiorgis, P. Delsanto, P. Gabriele, T. Deisboeck, Does tumor growth follow a 'universal law'? J. Theor. Biol. 225 (2003) 147–151.
[16] P. Castorina, P. Delsanto, C. Guiot, A classification scheme for phenomenological universalities in growth problems in physics and other sciences, Phys. Rev. Lett. 96 (2006), doi:10.1103/PhysRevLett.96.188701.
[17] G. West, J. Brown, B. Enquist, A general model for ontogenetic growth, Nature 413 (2001) 628–631.
[18] C. Guiot, N. Pugno, P. Delsanto, T. Desiboeck, Physical aspect of cancer invasion, Phys. Biol. 4 (2007) 1–6, doi:10.1088/1478-3975/4/4/P01.
[19] P. Delsanto, C. Guiot, P. Degiorgis, A. Condat, Y. Mansury, T. Desiboeck, Growth model for multicellular tumor spheroids, Phys. Lett. 85 (2004) 4225–4227.
[20] P. Castorina, D. Carcó, C. Guiot, T. Deisboeck, Tumor growth instability and its implications for chemotherapy, Cancer Res. 69 (2009) 8507–8515.
[21] A. Gliozzi, C. Guiot, P. Delsanto, D. Iordache, A novel approach to the analysis of human growth, Theor. Biol. Med. Modell. 9 (1) (2012) 1–16.
[22] L. Barberis, C. Condat, A. Gliozzi, P. Delsanto, Concurrent growth of phenotypic features: a phenomenological universalities approach, J. Theor. Biol. 264 (2010) 123–129.
[23] E. Venturino, S. Petrovskii, Recent Mathematical Models: A Synopsis, Aracne Editrice s.r.l., Roma, 2005.
[24] M. Kleiber, Body size and metabolism, Hilgardia 6 (11) (1932) 315–363.
[25] G. Dattoli, C. Guiot, P. Delsanto, P. Ottaviano, S. Pagnutti, T. Deisboeck, Cancer metabolism and the dynamics of metastasys, J. Theor. Biol. 256 (2009) 305–310.
[26] G.S. Stamatakos, E. Kolokotroni, D. Dionysiou, C. Veith, Y. Kim, A. Franz, K. Marias, J. Sabczynski, R. Bohle, N. Graf, In silico oncology: Exploiting clinical studies to clinically adapt and validate multiscale oncosimulators, in: Proceedings of the Annual International Conference of the IEEE Engineering in Medicine and Biology Society, EMBS, 2013, pp. 5545–5549.
[27] D. Gabriele, F. Porpiglia, G. Muto, P. Gontero, C. Terrone, S. Annoscia, D. Randone, S. Benvenuti, G. Arena, I. Stura, C. Guiot, Eureka-1 database: an epidemiogical analysis, Minerva Urol. Nefrol. 1 (1) (2015) 9–15.